ORAL REFERENCE: ICF100362OR

NUMERICAL SIMULATION OF CRACK TIP FIELDS AND TOUGHENING MECHANISMS IN TERNARY POLYMER BLENDS

Th. Seelig[1], E. van der Giessen[2] and D. Gross[1]

[1]Institute of Mechanics, TU Darmstadt, D-64289 Darmstadt, Germany
[2]Micromechanics of Materials Group, University of Groningen, 9747 AG Groningen, The Netherlands

ABSTRACT

Crack tip fields in ternary polymer blends of PC/ABS are investigated numerically to address the effect of various microstructural features on the fracture initiation toughness. Under global small-scale yielding conditions, two-dimensional (2D) plane strain finite element analyses are carried out for the crack tip region featuring a process zone in which the blend microstructure is explicitly represented. The constitutive model accounts for large visco-plastic strains, the intrinsic softening-rehardening behavior of glassy polymers as well as plastic dilatation in the ABS phase due to rubber particle cavitation. Attention is focused on the influence of the blend composition and morphology on the competition between crazing and shear yielding in the PC matrix. A set of indicators is used to classify various blends with respect to their tendency to enhance toughness.

KEYWORDS

Polymer blends, toughening mechanisms, crack tip plasticity, craze initiation, rubber cavitation, morphology

INTRODUCTION

Although amorphous thermoplastics, such as polycarbonate (PC), are able to undergo large inelastic deformations under, for example, compression, they show a strong notch sensitivity. The reason is the concentration of hydrostatic stress ahead of crack tips or notches which may initiate brittle failure by ‘crazing’. Blending these materials with small rubber particles is a well-established route to increase their fracture toughness. The key mechanism for toughening is understood to be rubber particle cavitation, which delays crazing due to the relief in hydrostatic stress and promotes plastic flow (‘shear yielding’) in the matrix, hence increases energy absorbtion [1].

The class of ‘ternary’ blends like PC/ABS is much less well understood. In these materials, ABS (acrytonitril-butadiene-styrene) is itself a blend of SAN (styrene-acrytonitril, another thermoplastic) and rubber (butadiene) particles. A toughening effect is again attributed to rubber particle cavitation in the ABS phase and enhancement of shear yielding in the PC matrix [2,3]. However, the situation is complicated by several additional parameters (ABS composition, blend morphology) and additional mechanisms (multiple crazing in ABS, interface debonding). For example, there seems to be no clear consensus yet how the frequently reported ‘syn-

ergistic effect' of a maximum toughness of the blend at an ABS content of around 20 - 30 % depends on the ABS microstructure (e.g. rubber content), and experimental findings sometimes are contradictory [3]. Equally unclear is the influence of the blend morphology (particulate vs oriented ABS layers). The purpose of the present numerical investigation is to gain some basic insight into the role these parameters play in the process of toughening.

Earlier theoretical work has mainly focused either on crack tip fields (e.g. evolution of plastic zone) in homogeneous material [4,5] or on cell studies of blends (with rubber particles treated as voids) under uniform macroscopic load [6,7]. The latter type of modeling clearly revealed the enhanced plastic flow in blends by shear banding between the modifier particles as well as a reduction of hydrostatic stress. Chen and Mai [8] investigated a 3D model of a rubber particle interacting with a crack tip in PC described as a standard von Mises material. The present work is a first step to study the characteristic behavior of (ternary) polymer blends under loading conditions prevailing at crack tips. Since no failure mechanism is accounted for, we are concerned only with the situation prior to crack advance and implications on the fracture initiation toughness. We do so in a 2D plane strain model of a crack tip in PC surrounded by several ABS particles and study the spreading of the plastic zone (e.g. by shear banding between interacting particles), the stress distribution and the dissipated work. These characteristics are discussed in relation to the toughening effect of the blend composition and morphology.

PROBLEM FORMULATION

Since the inelastic processes to be investigated are localized at the tip of a pre-crack or notch small-scale yielding is assumed and only the K-field dominated region is modeled (Fig. 1a). Mode I loading is imposed in terms of the respective displacements as far-field boundary conditions (cf. [4,5]). A closer look at the crack tip (which then appears blunted) reveals the microstructure of the blend as a two-phase material with a PC matrix and ABS particles (Fig. 1a). At this level, i.e. in the so-called 'process zone', both phases are described as homogeneous materials by constitutive equations given in the next section. The even finer ABS microstructure of small rubber particles in a SAN matrix is only considered in a homogenized sense.

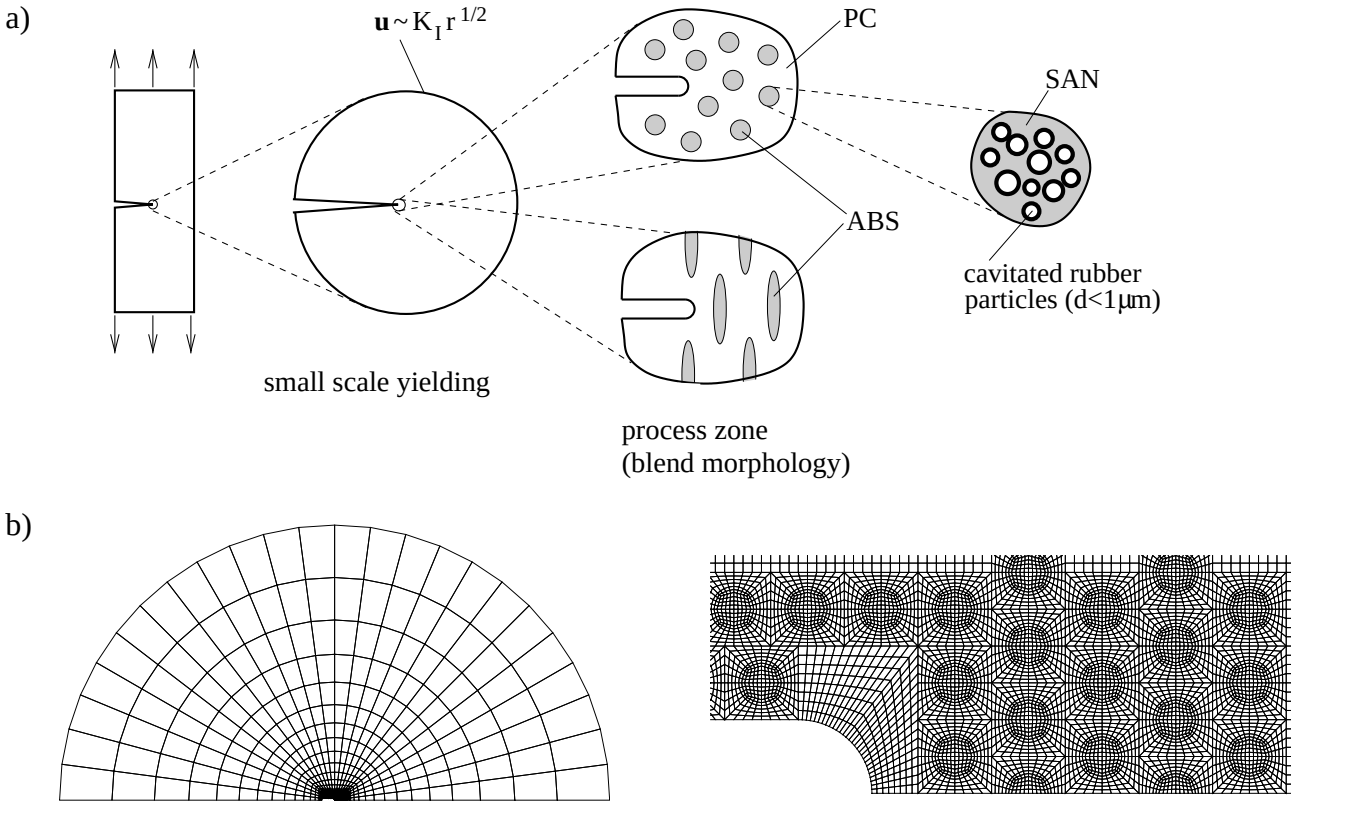

Figure 1: a) Crack tip modeling in ternary polymer blend. b) Finite element discretization of crack tip region and example of process zone (inner mesh).

Quasistatic loading of the crack tip region takes place at a prescribed constant rate $\dot{K}_I$. Details on the incremental solution procedure may be found in [4]. The finite element meshes used in a number of analyses to be presented are depicted in Fig. 1b, where the process region mesh (Fig. 1b, right) shows one of several investigated cases. Exploiting the symmetry of the model, only half of the problem has to be discretized.

CONSTITUTIVE EQUATIONS

The deformation behaviour of glassy polymers like PC or SAN is described by the same elastic visco-plastic constitutive model used in [4]. It employs a standard additive decomposition of the rate of deformation tensor into its elastic and plastic parts: $\boldsymbol{D} = \boldsymbol{D}^{\mathrm{e}} + \boldsymbol{D}^{\mathrm{p}}$. Since the elastic strains remain small they are governed by Hooke's law which in rate form can be written as $\boldsymbol{D}^{\mathrm{e}} = \boldsymbol{\mathcal{L}}^{-1} \overset{\triangledown}{\boldsymbol{\sigma}}$ where $\overset{\triangledown}{\boldsymbol{\sigma}}$ is the Jaumann rate of the Cauchy stress $\boldsymbol{\sigma}$, and $\boldsymbol{\mathcal{L}}$ is the standard fourth order isotropic elasticity tensor.

Matrix behavior
Rate-dependent yielding of the matrix material is specified through the visco-plastic constitutive equations

$$\boldsymbol{D}^{\mathrm{p}} = \frac{\dot{\gamma}^{\mathrm{p}}}{\sqrt{2}\tau}\bar{\boldsymbol{\sigma}}', \quad \dot{\gamma}^{\mathrm{p}} = \sqrt{\boldsymbol{D}^{\mathrm{p}} \cdot \boldsymbol{D}^{\mathrm{p}}}\,, \quad \tau = \sqrt{\frac{\bar{\boldsymbol{\sigma}}' \cdot \bar{\boldsymbol{\sigma}}'}{2}}\,, \quad \dot{\gamma}^{\mathrm{p}} = \dot{\gamma}_0 \exp\left[-\frac{As}{T}\left(1 - \left(\frac{\tau}{s}\right)^{5/6}\right)\right], \tag{1}$$

based on the equivalent plastic shear strain rate $\dot{\gamma}^{\mathrm{p}}$ being determined by the equivalent driving shear stress τ, with $\dot{\gamma}_0$ and A material parameters, and T the absolute temperature. Softening of the material upon yield is accounted for by the yield resistance s evolving with plastic strain, while rehardening due to stretching of the molecular network is described by the back stress tensor $\boldsymbol{b}$ incorporated in the purely deviatoric driving stress tensor $\bar{\boldsymbol{\sigma}}' = \boldsymbol{\sigma}' - \boldsymbol{b}$ (see [4] for details).

Homogenized ABS behavior
Once the rubber particles in the ABS phase have cavitated they are mechanically equivalent to voids because of the low modulus of the rubber. The overall behavior of ABS can then be approximated by that of porous SAN. The elasticity tensor now is expressed in terms of effective (e.g. Mori-Tanaka) elastic constants $\boldsymbol{\mathcal{L}}(f)$ where f is the porosity [9]. To allow for yielding of the porous material under deviatoric and hydrostatic stress states the equivalent driving stress τ in (1) is taken to be related to the deviatoric driving stress $\bar{\boldsymbol{\sigma}}'$ and the mean stress σ_m via the phenomenological macroscopic yield function

$$\Phi \equiv \frac{1}{2}\bar{\boldsymbol{\sigma}}' \cdot \bar{\boldsymbol{\sigma}}' + a f_0^b \sigma_m^2 - [(1-f)\tau c(f_0)]^2 = 0\,. \tag{2}$$

Here, a and b are 'pressure sensitivity' parameters to be fitted from cell calculations for porous SAN and f_0 is the initial porosity (rubber content in ABS). With $1-f$ being the volume fraction of the matrix material, $(1-f)\tau c(f_0)$ can be regarded as the equivalent driving stress of the porous material where the factor $c(f_0)$ accounts for initially localized yielding in the intervoid ligament discussed in [9]. For example, the equivalent driving stress initially, i.e. for $f = f_0$, is $(1-\sqrt{f_0})\tau$, if $c(f_0) = (1+\sqrt{f_0})^{-1}$ is chosen for the 2D case of cylindrical voids. In this case, the factor $1-\sqrt{f_0}$ is approximately the relative width of the ligament between voids where plastic flow is localized at the onset of macroscopic yield.
The function Φ serves to determine the driving stress τ (from $\Phi = 0$) as well as the plastic strain rate via the normality rule $\boldsymbol{D}^{\mathrm{p}} = \Lambda \partial\Phi/\partial\bar{\boldsymbol{\sigma}}$. The multiplier Λ is computed from the condition that the plastic work rate per unit volume in the porous material equals the dissipation in the matrix: $\bar{\boldsymbol{\sigma}} \cdot \boldsymbol{D}^{\mathrm{p}} = (1-f)\sqrt{2}\tau\dot{\gamma}^{\mathrm{p}}$.

CRAZE INITIATION

Crazing in the PC matrix can be regarded as a precursor of brittle failure of the blend material. Beside craze growth and final breakdown, the initiation phase is probably the least well understood part of this process

[10]. Since craze formation starts with microvoiding, the hydrostatic stress certainly plays a crucial role, and attainment of a critical value of σ_m can serve as a simplest initiation criterion [7]. Other criteria, as discussed by Estevez et al. [5], also incorporate shear stress due to the need for some plastic deformation. For example, the criterion of Sternstein (see [5]) can, under plane strain conditions, be cast into the form $F_c \equiv 2\tau - B_0/3\sigma_m + A_0 = 0$ where A_0 and B_0 are material parameters. No reliable data for craze initiation in PC are available yet. So, to compare various blends with regard to their tendency to matrix crazing we simply trace the peak values of σ_m and F_c attained in the PC phase in the course of a loading process. The experimental observation that highly stretched material is less prone to craze [10] is accounted for by recording $\sigma_m^{\max}$ and $F_c^{\max}$ only in material undergone a maximum stretch of less than 2.

RESULTS

All results to be presented have been obtained at a constant loading rate of $\dot{K}_I = 1\text{MPa}\sqrt{\text{m}}\text{sec}^{-1}$. Typical values for the material parameters of PC and SAN are taken from [6]. From cell studies for porous SAN (not reported here for brevity) the pressure sensitivity parameters in the yield function (2) have been determined to be $a = 1.0$ and $b = 0.7$. Based on the case study in [5] the values for the parameters entering the craze initiation criterion are chosen to be $A_0 = 0.7s_0$ and $B_0 = 3s_0^2$ where $s_0 \approx 100$MPa is the initial yield strength of PC. A dimensionless applied stress intensity factor $\bar{K}_{\text{app}}$ is defined by dividing K_I by $s_0\sqrt{r_{\text{tip}}}$ where r_{tip} is the crack tip radius, and $\bar{W}_{\text{diss}}$ denotes the dissipated work normalized by $s_0 r_{\text{tip}}^2/25$.

Effect of Morphology

The effect of the morphology of the ABS phase (in either case 30% ABS with 10% rubber) is illustrated in Fig. 2 showing the spreading of the plastic zone in terms of the equivalent plastic strain rate $\dot{\gamma}^{\text{p}}$. While plastic flow in homogeneous PC is highly localized in form of narrow shear bands intersecting ahead of the blunt crack tip [4], the presence of ABS causes far more distributed yielding. In the case of the blend with spherical ABS particles, one observes shear banding in the PC matrix between these particles. In the microstructure with ABS layers (highly elongated particles) perpendicular to the crack the plastic zone extends ahead of the crack tip and successively spreads along the layers.

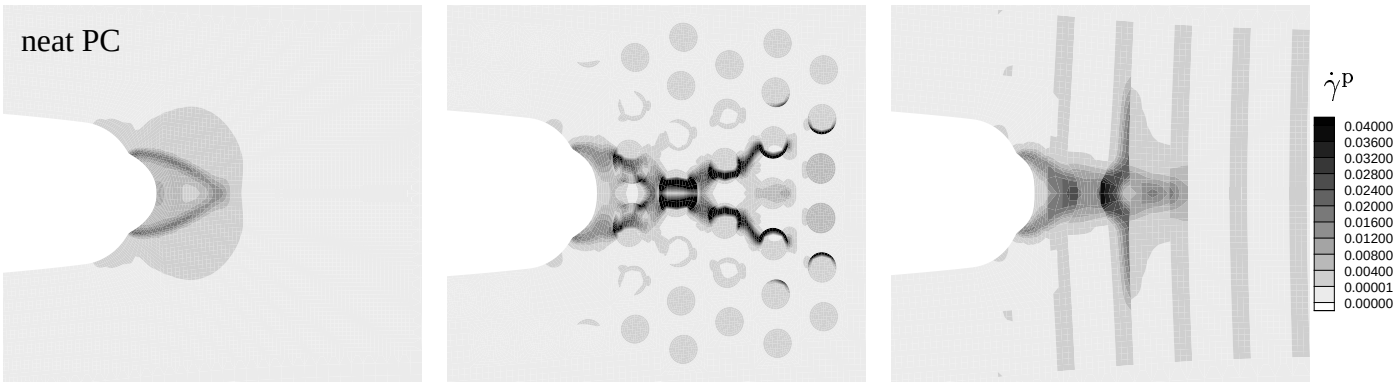

Figure 2: Equivalent plastic strain rate $\dot{\gamma}^{\text{p}}$ [sec^{-1}] at $\bar{K}_{\text{app}} = 2.25$; 30% ABS containing 10% rubber

The distribution of hydrostatic stress shown in Fig. 3 is seen to be less localized in case of the blends, possibly leading to a more distributed matrix failure and hence higher toughness. For both morphologies, σ_m in the ABS phase at locations further away from the crack tip is higher than in the surrounding PC matrix because of the higher elastic stiffness of ABS at low rubber content. The opposite can be seen inside the plastic zone where the capacity of ABS to carry hydrostatic stress has strongly decreased due to volumetric yielding. Hydrostatic stress is then concentrated in the PC matrix. Close to the crack tip volumetric expansion of the ABS material is quite pronounced and accompanied by necking of the PC ligament.

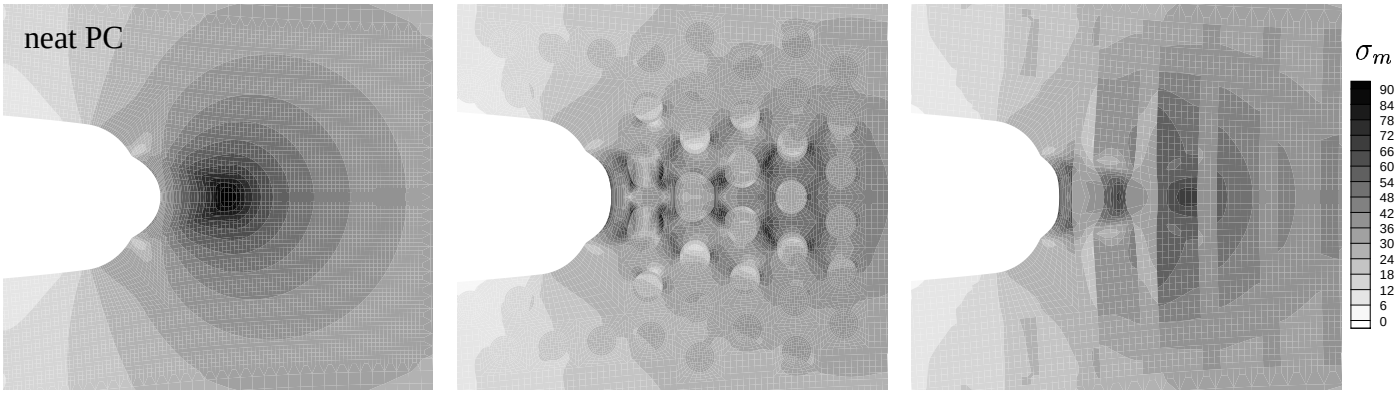

Figure 3: Hydrostatic stress σ_m [MPa] at $\bar{K}_{\text{app}} = 2.25$; 30% ABS containing 10% rubber

The influence of the microstructure is analyzed and compared to the situation in neat PC in terms of the dissipated work $\bar{W}_{\text{diss}}$ and the peak values (attained somewhere in the process zone) of hydrostatic stress $\sigma_m^{\max}$ and of the craze initiation indicator $F_c^{\max}$ as functions of the applied stress intensity factor. To smooth out local effects resulting only from a particular arrangement of the ABS particles around the crack tip, an 'ensemble averaging' over three different arrangements (realizations of statistically the same microstructure) is performed.

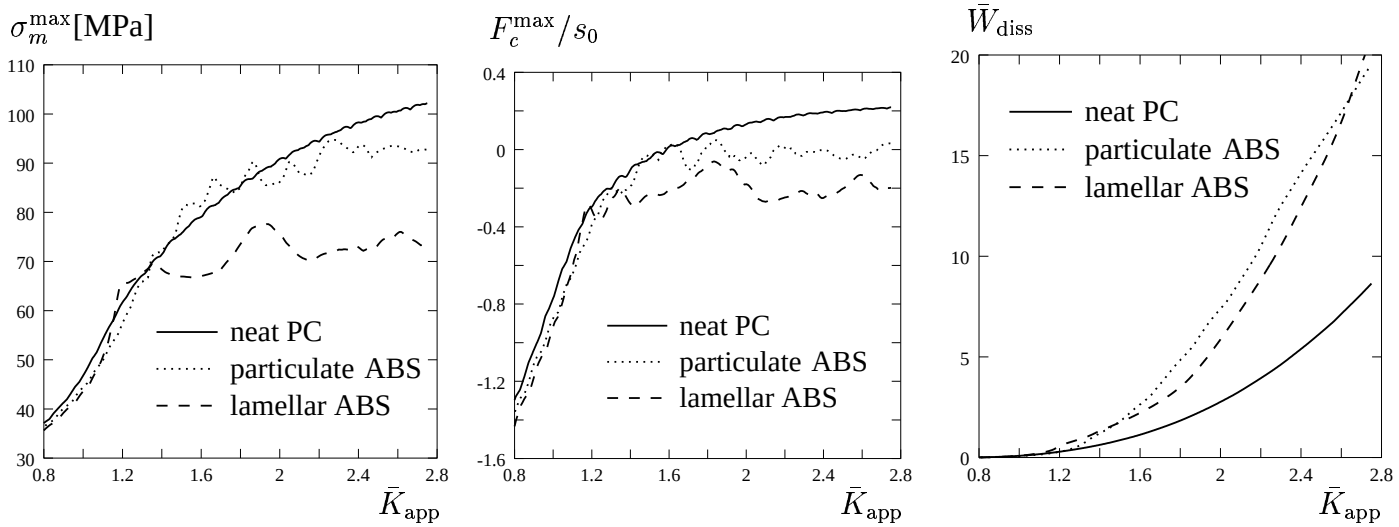

Figure 4: Effect of morphology; 30% ABS containing 10% rubber

From Fig. 4 we see that in both blends the peak values of hydrostatic stress and the craze initiation indicator are lower than in neat PC while the absorbed energy is significantly higher. This suggests that both blends should be expected to be significantly tougher than neat PC. However, which one of the two morphologies is more efficient is less clear; the lamellar microstructure yields lower values for the stress-based criteria whereas the particulate microstructure absorbs slightly more energy. It should be mentioned that the morphologies investigated here may prevail in real materials at different ABS content, with a higher volume fraction leading to a lamellar microstructure, at least for injection moulding [3].

Effect of Rubber Content in ABS

Another important parameter in the fracture behavior of PC/ABS blends is the rubber content in the ABS phase [2,3]. For a blend containing a volume fraction of 30% spherical ABS particles, the effect of the rubber content is shown in Fig. 5. Again, results are compared to those for neat PC. The extreme case of 0% rubber is in fact a blend of PC and SAN which – from the indicators inspected here – seems to yield no toughening effect. The addition of some rubber leads to a much higher energy dissipation and lower values of hydrostatic stress and the craze initiation indicator. Doubling the amount of rubber in ABS results only in a small improvement.

A similar ‘saturation’ effect has been observed when varying the ABS volume fraction in the blend at fixed rubber content.

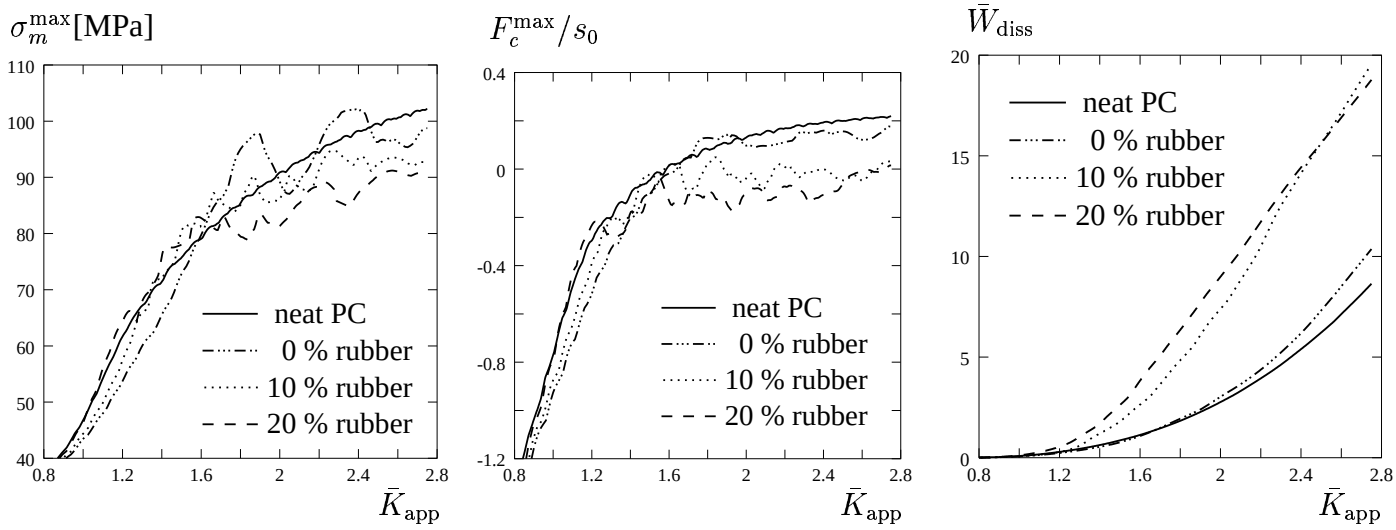

Figure 5: Effect of rubber content in ABS; 30% spherical particles

CONCLUSIONS

Crack tip fields in PC/ABS blends prior to crack growth have been simulated and analyzed with respect to their dependence on characteristic features of the microstructure, such as morphology and composition. Enhanced plastic flow and dissipation as well as the redistribution of stress with reduced peak values in case of blends could be interpreted as contributing to toughening compared to homogeneous PC. However, comparison with experimental observation has to be taken with caution since the occurrence of failure mechanisms, such as crazing, have been ignored here. It is possible that toughening mechanisms fully develop only during crack advance and are active mainly in the wake region of the crack as discussed in [6,11].

REFERENCES

1. Bucknall, C.B. (1997). In: *The Physics of Glassy Polymers*, pp. 363-412, Haward, R.N. and Young, R.J. (Eds.). Chapman & Hall, London.
2. Ishikawa, M. (1995) *Polymer* 36, 2203.
3. Greco, R. (1996). In: *Advanced Routes for Polymer Toughening*, pp. 469-526, Martuscelli, E., Musto, P. and Ragosta, G. (Eds.). Elsevier.
4. Lai, J. and van der Giessen, E. (1997) *Mech. Mater.* 25, 183.
5. Estevez, R., Tijssens, M.G.A. and van der Giessen, E. (2000) *J. Mech. Phys. Solids* 48, 2585.
6. Pijnenburg, K.G.W., Steenbrink, A.C. and van der Giessen, E. (1999) *Polymer* 40, 5761.
7. Socrate, S. and Boyce, M.C. (2000) *J. Mech. Phys. Solids* 48, 233.
8. Chen, X.-H. and Mai, Y.-W. (1999) *J. Mat. Sci.* 34, 2139.
9. Pijnenburg, K.G.W. and van der Giessen, E. (2001) *Int. J. Solids Struct.* 38, 3575-3598.
10. Donald, A.M. (1997). In: *The Physics of Glassy Polymers*, pp. 295-341, Haward, R.N. and Young, R.J. (Eds.). Chapman & Hall, London.
11. Thouless, M.D., Du, J. and Yee, A.F. (2000). In: *Toughening of Plastics*, pp. 71-85, Pearson, R.A., Sue, H.-J. and Yee, A.F. (Eds.). American Chemical Society, Washington DC.